

EUROPEAN ORGANIZATION FOR NUCLEAR RESEARCH

CERN - AB Department

CERN-AB-2008-022

CLIC-Note -761

EUROTeV-Report-2008-035

BEAM DYNAMICS ISSUES IN THE CLIC LONG TRANSFER LINE*

J.B. Jeanneret, E. Adli, A. Latina, G. Rumolo, D. Schulte and R. Tomas

CERN, Geneva, Switzerland

Abstract

Both the main and the drive beam of the CLIC project must be transported from the central production site to the head of the main linacs over more than twenty kilometers. Over such distances chromatic error may be substantial. With long distances and large beam currents, ion-induced detuning and instabilities and multi-bunch resistive wall effects must also be considered. These effects are quantified and simulated. Based on these results, a baseline design has been established.

CERN-AB-2008-022



*Work supported by the Commission of the European Communities under the 6th Framework Programme "Structuring the European Research Area", contract number RIDS-011899.

Presented at
EPAC'08, 11th European Particle Accelerator Conference, Genoa, Italy - June 23-27, 2008

*Geneva, Switzerland
August 2008*

BEAM DYNAMICS ISSUES IN THE CLIC LONG TRANSFER LINE

J.B. Jeanneret, E. Adli, A. Latina, G. Rumolo, D. Schulte, R. Tomas, CERN, Geneva, Switzerland*

Abstract

Both the main and the drive beam of the CLIC project must be transported from the central production site to the head of the main linacs over more than twenty kilometers. Over such distances chromatic error may be substantial. With long distances and large beam currents, ion-induced detuning and instabilities and multi-bunch resistive wall effects must also be considered. These effects are quantified and simulated. Based on these results, a baseline design has been established.

INTRODUCTION

In the CLIC project, the drive beam and the main beam will travel from their central production sites towards the head of the main linacs over $L > 20$ km. FODO cells can be used, but issues which are usually considered in rings must be addressed here because of the long distance. Optimized optics parameters are discussed in [1]. A phase-advance of $\Delta\psi_c = \pi/4$ minimizes the installed magnet power and the emittance growth due to quadrupole misalignment. Chromaticity is also kept small, but not enough to be negligible. We show below that the vacuum chamber must be large to limit resistive wall instabilities. This allows for using large beta-functions, thus minimizing further chromatic aberrations and emittance growth. We foresee a cell length of $L_{\text{cell}} = 438$ m for the main beam, limiting the total phase advance of the line to six periods. On the other hand, the drive beam must be matched to rather low β 's in the turnaround loops every $L_s = 877$ m. We foresee a cell length of $L_{\text{cell}} = 109.6$ m and one period per sector for a total phase advance of 24 periods. All the useful optics data can be found in Table 1 together with CLIC beam parameters [2]. We discuss below three issues which were identified as potential limitations for the performance of the project, namely chromatic aberrations, multi-bunch resistive wall instabilities and ion effects.

CHROMATIC EFFECTS

The momentum band of the two beams is large, i.e. $\hat{\delta}_p = 2\%$ (DB) and 1% (MB). With an even number of cells and thanks to the beta-beating phase running twice faster than the betatronic one, the chromatic Twiss error are quite small ($\Delta\beta/\beta < 3\%$ for the DB and $< 1\%$ for the MB), see figure 1. Transported to the downstream decelerator line, this error induces a marginal growth of the maximum beam size of 1% . On the other hand, the chromaticity grows linearly with the number of cells. With $C \simeq (L/2\pi\hat{\beta})(1 + \sin \frac{\psi_c}{2})/\cos \frac{\psi_c}{2}$, $C_{\text{DB}} = -21$ and

Table 1: Transfer Lines, Drive Beam and Main Beam data.

Parameter	Symbol	Value	Unit
Linac Length	L	21376	m
RF main frequency	ν_0	$1.2 \cdot 10^{10}$	Hz
Phase adv. /cell	$\Delta\psi_c$	$\pi/4$	rad
Drive Beam			
DB station length	L_s	877	m
Train length	l_t	73	m
Train-train gap	z_{tt}	1680	m
Bunch separation	$z_{\text{bb}} = c/\nu_0$	0.025	m
Bunch population	N	$5.25 \cdot 10^{10}$	-
Bunches per train	n	2900	-
Energy	E	2.5	GeV
Norm. emit.	$\epsilon_{n x,y}$	10^5	nm rad
Cell length	L_{cell}	109.6	m
Av. beta function	β	144	m
Total phase adv.	$\Delta\psi/2\pi$	24	-
Momentum band	$\hat{\delta}_p$	± 0.02	-
Main Beam			
Train length	l_t	48	m
Train-train gap	z_{tt}	1705	m
Bunch separation	$z_{\text{bb}} = 6c/\nu_0$	0.15	m
Bunch population	N	$4 \cdot 10^9$	-
Bunches per train	n	312	-
Energy	E	9	GeV
Norm. emit. x,y	$\epsilon_{n x}, \epsilon_{n y}$	660, 20	nm rad
Cell length	L_{cell}	438	m
Av. beta function	β	575	m
Total phase adv.	$\Delta\psi/2\pi$	6	-
Momentum band	$\hat{\delta}_p$	± 0.01	-

$C_{\text{MB}} = -5.3$. For the DB this converts to $2\pi\hat{\delta}_p C \simeq 155^\circ$. This is large enough to nearly fully filament the beam in case of injection and kick errors. This may prevent to diagnose the latter effect in view of the difficulty to measure the beam size in production conditions. This also precludes the use of a correction system implemented downstream. A chromatic correction may solve this problem, but with some added complexity. The case of Main Beam is more favorable with a small $2\pi\hat{\delta}_p C \simeq 18^\circ$.

RESISTIVE WALL INSTABILITY

With dense and long trains, the transverse resistive wall impedance is large. For the multi-bunch effect we use the long-distance formula which expresses the dipole moment of the impedance per longitudinal unit length [3]

$$w_{\perp}(z) = \frac{\Delta_x(s)c}{\pi a^3} \sqrt{\frac{Z_0}{\pi\sigma}} z^{-1/2} \quad (\text{S.I. units}) \quad (1)$$

* Work supported by the Commission of the European Communities under the 6th Framework Programme Structuring the European Research Area, contract number RIDS-011899.

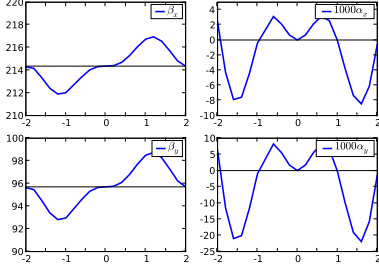


Figure 1: Chromatic variation of the Twiss functions at the end of the Drive Beam line for a momentum band of 2%.

with $\Delta_x(s)$ the transverse displacement of a bunch at the position s along the beam line, z the distance from any bunch to the last one of the train, a the vacuum chamber radius and σ its electrical conductivity. With the beam energy E in [eV], the transverse kick per meter of beam line and per bunch of population N is

$$\frac{dx'^2}{dsdz} = \frac{dE_{\perp}}{eE} = N ew_{\perp}(s, z) \quad (2)$$

In a small kick approximation, the whole train is rigid, except for the last bunch. With $z_i = iz_{bb}$ the distance from the bunch of index $n - i$ to the last one of index n and summing over i , the kick per meter is

$$\frac{dx'_n}{ds} = \frac{new_{\perp}(s)}{E\sqrt{z_{bb}}} \sum_{i=1}^{n-1} i^{-1/2} \simeq \frac{2new_{\perp}(s)}{E} \sqrt{\frac{n-1}{z_{bb}}} \quad (3)$$

The integral over $s \in [0, L]$ is approximated by splitting the line in $M = L/l$ elements in which $\Delta_x = |\langle \Delta_x(s) \rangle| \simeq \text{cst}$ is used as an r.m.s. value. The kick induces a displacement at $s = L$

$$\delta x = \frac{dx'_n(\Delta_x)}{ds} l \sum_{j=1}^M \sqrt{\beta_i \beta} \sin \mu_j \quad (4)$$

After quadratic summing and with $l = L/M$,

$$\langle \delta x^2 \rangle^{1/2} = \frac{dx'_n(\Delta_x)}{ds} \sqrt{\frac{Ll\bar{\beta}\beta}{2}} \quad (5)$$

The normalizing displacement $\delta A_n = \sqrt{\langle \delta x^2 \rangle / \epsilon \beta}$ is

$$\delta A_n = \Delta_x \sqrt{\frac{2(n-1)\bar{\beta}LlZ_0}{\pi \epsilon z_{bb} \sigma} \frac{Nec}{\pi a^3 E}}. \quad (6)$$

Some results are quoted in Table 2 for a copper vacuum chamber with a resistivity $\sigma_{Cu} = 5.9 \cdot 10^7 \Omega^{-1}m^{-1}$ of radius $a = 0.1$ m for the Drive Beam and $a = 0.06$ m for the Main Beam. The emittance growth and the amplification of injection errors are adequately small. A large copper chamber is indeed mandatory. With stainless steel ($\sigma_{ss} = 1.4 \cdot 10^6 \Omega^{-1}m^{-1}$), the minimum radius would be $a_{ss} \simeq (\sigma_{Cu}/\sigma_{ss})^{1/6} a_{Cu} = 1.85 a_{Cu}$.

Table 2: Normalized emittance growth of the trailing bunches associated to multi-bunch resistive wall effect for three different sources of transverse displacements with a **copper chamber of radius $a = 0.1$ m for the Drive Beam and $a = 0.06$ m for the Main Beam**. $\delta\epsilon_n$ applies to both plane for the DB and to the vertical plane (worst case) for the MB. Emittances ϵ_n from Table 1. Results for injection errors are given as an amplification factor of the transverse injection error.

Source	Δ_x [m]	l [m]	$\delta\epsilon_n / \epsilon_n$ [nm rad]
Drive beam			
CO error, rms	10^{-3}	$L_{\text{cell}}/2$	$4 \cdot 10^3 / 10^5$
Vac. ch. error	$3 \cdot 10^{-3}$	10	$5 \cdot 10^3 / 10^5$
Main beam			
CO error, rms	10^{-3}	$L_{\text{cell}}/2$	$5.6 / 20$
Vac. ch. error	$3 \cdot 10^{-3}$	10	$3.6 / 20$
Source	$\Delta_{x,y}^{\text{in}} / \sigma_{\beta_{x,y}}$	l [m]	$\Delta_{x,y}^{\text{out}} / \sigma_{\beta_{x,y}}$
Injection error			
Drive beam	1	L	1.1
Main beam	1	L	1.03

ION EFFECTS

Electron or positron beams ionize the residual gas on their path. With electrons beams, the electrons of the ionized gas are repelled while the positively charged ions can be trapped inside the beam. Conversely, with a positron beam, ions are repelled while electrons can be trapped.

Electron Beams

The ion density grows linearly at the passage of a train. Its maximum longitudinal density at the end of the train is $\lambda_{\text{ion}} = nN\rho_{\text{gas}}\sigma_{\text{ion}}$, with $\rho_{\text{gas}} = 3.54 \cdot 10^{22} p$ [mol/m³, Torr] and the ionization cross-section [4]

$$\sigma_{\text{ion}} = 4\pi \left(\frac{\hbar}{m_e c} \right)^2 \beta^2 [C_1 + 2C_2(\ln \beta\gamma - 0.5)] \quad (7)$$

The ions can be trapped in the potential of the electron beam if their atomic number A is large enough. Under a critical value A_{trap} , the ions are overfocused [4]. The trapping condition [4]

$$A > A_{\text{trap}} = \frac{16Q_i r_p \tilde{n} \Delta z}{3\pi^2 (\sigma_x + \sigma_y) \sigma_y} \quad (8)$$

is given by the limit of stability of the ions in the focusing structure of either the bunches inside a train ($\Delta z = z_{bb}$, $\tilde{n} = N$, critical $A = A_{bb}$) or the train structure with their gap ($\Delta z = z_{tt}$, $\tilde{n} = nN$, $A = A_{tt}$). In Eq. 8, $\sigma_{x,y}$ are the r.m.s. beam sizes and Q_i is the ion charge, with $Q_i = 1$ used here. Input variables are found in Table 1 and numerical results in Table 3. In high vacuum, the dominant gas is CO ($A = 28$) for which $C_1 = 35$, $C_2 = 3.7$. The

condition

$$A_{bb} < A < A_{tt} \quad (9)$$

is met for both beams, i.e. the ions are fully trapped in the trains, but disappear between trains, see Table 3. Trapped ions induce a betatron detuning and transverse instabilities. The detuning of the rear bunches is given by [5]

$$\Delta\nu_{x,y,inc} = \frac{\beta_{x,y} r_e Q_i \lambda_{ion} L}{2\pi\gamma\sigma_{x,y}(\sigma_x + \sigma_y)}. \quad (10)$$

This formula is obtained for a transverse distribution of the ions which is identical to the beam shape. This is an optimistic approximation. The ions are produced nearly at rest, i.e. their thermal momentum is negligible compared to their average momentum in oscillation in the beam potential. The result of a numerical simulation is shown in Fig. 2 for the drive beam, see [6] for a formal description. The most harmful central density is three times larger than in the case of a beam shaped ion distribution. A safe approach must therefore consider a detuning which is possibly three times larger than in Eq. 10. The rise-time of

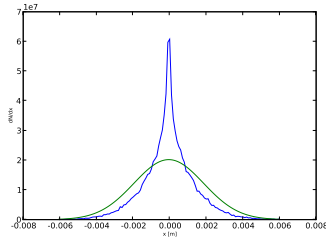


Figure 2: Ion asymptotic transverse distribution $dn/dx(y = 0)$ (blue) compared to the drive beam shape (red) in [a.u]. The distribution are normalized to each other. The scale of x is in m.

beam-ion instabilities is derived in [7] and re-expressed in a more compact form in [8] as

$$\tau_{rt} = \frac{\sqrt{18Q_i}(\sqrt{\epsilon_{nx} + \epsilon_{ny}} + \epsilon_{ny})aKT}{p\sigma_{ion}Nnr_e c} \quad (11)$$

with here p [N/m^2] = 129.1p [Torr]. The quantity a is a 'frequency factor', estimated to $a \simeq 0.1$ in [8]. In [7], it is shown that Eq. 11 underestimates the rise-time obtained with numerical simulation by a factor 2-3, while similarly large variations appear with different seeds. The number of rise-times $n_{rt} = L/(c\tau_{rt})$ across the line is therefore considered to be in the range $[n_{rt}, 3n_{rt}]$. The result given in Table 3 indicate that a pressure of $p \leq 10^{-10}$ Torr is mandatory to keep both $\Delta\nu$ and n_{rt} below unity in both beam lines.

Positron Beam

In the positron beam ionized electrons are not trapped in the trains, i.e. $m_e/m_p < A_{bb}$. Their precise fate remains to be checked, but we expect no problematic effects.

Table 3: Ion data

Parameter	Symbol	Value	Unit
Drive Beam			
Pressure	p	10^{-10}	Torr
Ion cross-section	σ_{ion}	$1.76 \cdot 10^{-22}$	m^{-2}
Max ion density	λ_{ion}	$9.5 \cdot 10^4$	m^{-1}
Trap. limit, bunches	A_{bb}	$1.9 \cdot 10^{-4}$	-
Trap. limit, trains	A_{tt}	$3.6 \cdot 10^4$	-
Incoh. detuning	$\Delta\nu_{x,y}$	[0.005 , 0.015]	-
Nb. of rise-times	n_{rt}	[0.06 , 0.18]	-
Main Beam			
Pressure	p	10^{-10}	Torr
Ion cross-section	σ_{ion}	$1.94 \cdot 10^{-22}$	m^{-2}
Max ion density	λ_i	$8.0 \cdot 10^2$	m^{-1}
Trap. limit, bunches	A_{bb}	$1.1 \cdot 10^{-2}$	-
Trap. limit, trains	A_{tt}	$3.7 \cdot 10^5$	-
Incoh. detuning	$\Delta\nu_y$	[0.06 , 0.17]	-
Nb. of rise-times	n_{rt}	[0.13 , 0.38]	-

SUMMARY

The long CLIC transfer lines require large radius copper chambers, respectively $a_{MB} = 60$ mm and $a_{DB} = 100$ mm. A very good residual pressure of $p \leq 10^{-10}$ T is mandatory. We note that the transfer lines from the surface down to the tunnel and the final turnarounds in the tunnel add several kilometers to the lines discussed here. Our conclusions apply to these as well. Chromatic effects are made small in the Main Beam by using long FODO cells, but may be problematic with respect to safe operation for the Drive Beam. In the latter case a chromatic correction system was studied and may be implemented. Finally, a beam-based alignment scheme remains to be implemented to minimize the effect of quadrupole misalignment.

REFERENCES

- [1] J.B. Jeanneret and H.H. Braun, Optimization of a FODO line, THPC017, these proc.
- [2] CLIC parameters 2008, CERN CLIC Note, F.Tecker ed., to be issued.
- [3] O.Henry, O.Napoly, The Resistive Wall Wake Potentials for short bunches, CERN CLIC Note 142 and DPhN/STAS/91-R08.
- [4] Y. Baconnier, Neutralization of Accelerator Beams by Ionization of the Residual Gas, CERN/PS/PSR 84-24, 1984.
- [5] F. Zimmermann, in Hand. of Acc. Phys and Eng, A.W. Chao, M.Tigner ed., World Scientific, 1998, p.128.
- [6] T.O. Raubenheimer, F.J. Decker, J.T. Seeman, Beam Distribution after Filamentation, PAC95, Dallas,1995.
- [7] F. Zimmermann, T.O. Raubenheimer, G. Stupakov, A Fast Beam-ion Instability, PAC95, Dallas,1995.
- [8] T.O. Raubenheimer, D. Schulte, Fast Beam-ion Instability in CLIC, unpublished, 1999.
- [9] T.O. Raubenheimer, Ion effects in Future Circular and Linear Colliders, PAC95, Dallas,1995.